Chemical Engineering Journal 241 (2014) 336–343

Contents lists available at ScienceDirect

Chemical Engineering Journal

journal homepage: www.elsevier.com/locate/cej

High catalytic activity at low temperature in oxidative dehydrogenation of propane with Cr–Al pillared clay

María Andrea De León [a,*], Carolina De Los Santos [a], Luis Latrónica [a], Ana María Cesio [b], Cristina Volzone [b], Jorge Castiglioni [a], Marta Sergio [a]

[a] Laboratorio de Fisicoquímica de Superficies, Facultad de Química, Universidad de la República, CC 1157, CP 11800 Montevideo, Uruguay
[b] Centro de Tecnología de Recursos Minerales y Cerámica, CETMIC (CCT CONICET La Plata –CICPBA), CC 49, Camino Centenario y 506, (1897) M.B. Gonnet, Prov. Buenos Aires, Argentina

HIGHLIGHTS

- A montmorillonite was pillared with Al and/or Cr and tested in ODP.
- All catalysts (Al–C, Cr–C, Al–Cr–C) were active in ODP.
- The highest propylene yield (10.3%) was obtained with the Al–Cr–C catalyst at 450 °C.
- Even at 350 °C a promising propylene yield of 9.3% was obtained with Al–Cr–C.

ARTICLE INFO

Article history:
Received 17 June 2013
Received in revised form 8 October 2013
Accepted 29 October 2013
Available online 6 November 2013

Keywords:
Oxidative dehydrogenation
Propane
Propene
Al–Cr-PILC

ABSTRACT

A montmorillonite was pillared separately with chromium and aluminum polyoxocations (Cr–C and Al–C respectively) and also with an equimolar mixture of both polioxocations (Al–Cr–C). The resulting solids were characterized by scanning electron microscopy, energy dispersive spectrometry, thermal analysis, Fourier transform infrared spectroscopy, X-ray diffraction and nitrogen adsorption at −196 °C. The inclusion of polycations in the interlamellar space led to modifications in the properties of the clay. An eleven fold increase in specific surface area with respect to the calcined starting clay was found for the Al–C, whereas a twofold increase was observed for the Cr–C; the value for the Al–Cr–C was only slightly higher than that for the latter. Diffractograms of the Cr–C showed the occurrence of a Cr_2O_3 phase. Catalytic activity in oxidative dehydrogenation of propane was assayed in the temperature range from 350 °C to 450 °C using $Ar/C_3H_8/O_2$ (80/10/10) as reactant gas mixture. Propylene selectivity was found to be temperature-dependent, showing a maximum in the studied temperature range for the catalyst containing only aluminum, whereas remaining practically constant for the Cr-containing catalysts. Highly promising propylene yields at low temperature were obtained with the catalyst containing Al and Cr (Al–Cr–C): 9.3% at 350 °C and 10.3% at 450 °C.

1. Introduction

Light alkanes, including propane, are abundant in natural gas and as by-products of oil refining and are commercialized mainly for their fuel value. Their transformation into the corresponding olefins, via dehydrogenation or oxidative dehydrogenation, converts them into raw materials for petrochemical industry, thus increasing dramatically their value. Particularly for propane an industrial process has not yet been developed as Cavani et al. [1] assure in a recent review on the topic. The authors conclude: "it is evident that, in the future, the greatest efforts will be devoted to the study of catalysts and/or reactor configurations that are capable of maintaining high selectivity to propylene under conditions leading to high propane conversion". In consequence the researchers' attention is focused still nowadays on the topic.

Dehydrogenation so well as oxidative dehydrogenation is thermodynamically favorable and for propane the reactions are as follows:

$$C_3H_8 \rightarrow C_3H_6 + H_2 \qquad \Delta H_{298} + 124\ \text{kJ mol}^{-1}$$

$$C_3H_8 + 1/2O_2 \rightarrow C_3H_6 + H_2O \quad \Delta H_{298} = 117\ \text{kJ mol}^{-1}$$

Catalytic propane dehydrogenation requires high temperature (over 700 °C) to attain propene yields that assure the economic balance of the process. In these conditions coke deposition on

* Corresponding author. Tel./fax: +598 29241906.
E-mail addresses: adeleon@fq.edu.uy (M.A. De León), cdlsantos@fq.edu.uy (C. De Los Santos), llatroni@latu.org.uy (L. Latrónica), amcesio@speedy.com.ar (A.M. Cesio), volzcris@netverk.com.ar (C. Volzone), jcastig@fq.edu.uy (J. Castiglioni), msergio@fq.edu.uy (M. Sergio).

1385-8947/$ - see front matter © 2013 Elsevier B.V. All rights reserved.
http://dx.doi.org/10.1016/j.cej.2013.10.086

the catalyst is unavoidable requiring regenerations cycles to restore catalyst activity [2–4]. Oxidative dehydrogenation of propane (ODP) allows comparable yields at relative lower temperatures (under 600 °C) which in addition to the presence of oxygen in the reaction mixture diminish the risk for coke deposition. The use of lower temperatures and the fact to avoid regeneration cycles contribute to the economy of the process. As the reaction is exothermic high temperatures are reached during the process, that although favorable from a kinetic point of view, they contribute to undesired side reactions as cracking and total oxidation of reactants and products.

As an extra drawback the high temperatures compromise the catalyst structure in detriment of the catalytic performance [5]. Finding a highly active catalyst at low temperature or even at moderate temperatures –but not compromising catalyst's structure– represents a great challenge nowadays. The catalytic activity of chromium in paraffin dehydrogenation –especially C_3 and C_4– for olefin production has been reported. Generally the active species is supported on a solid having a high specific surface area as alumina [6–8], silica [9,10] mesoporous solids [11] and microporous materials [12].

Clays, due to their abundance and low cost, are interesting materials to be used in catalysts synthesis. Their low specific surface area represents a drawback for their direct application. However the smectites, particularly montmorillonites, owing to their high exchange capacity and expandable character, can be transformed into solids with high microporosity and specific surface area, which are referred to as pillared clays (PILC: Pillared Inter Layered Clay). The pillaring technique involves the exchange of the interlayer cations of the clay by bulky ones; the subsequent controlled calcination leads to the formation of oxidic species between the clay layers [13] and generates an open and rigid structure. Polioxocations of aluminum, known as Al_{13}, have been widely used to prepare alumina-pillared clays (Al-PILCs), also polyhydroxy species of Fe, Ti, Cr, Ga as well as of mixed metal cations have been reported and are summarized in comprehensive reviews [14–16]. An improvement of Al-PILCs thermal stability was verified when the polioxocation was prepared by basic hydrolysis of a solution containing Ga and Al in a ratio of 1:12 [17].

Preparation of chromium-polioxocations has been reported by several authors [18–20] and has enabled the synthesis of chromium-pillared clays (Cr-PILCs) [21–28]. Heat treatment conditions –temperature and atmosphere– influence greatly the structural and textural properties of these solids. Most authors report that the basal spacing (d_{001}) achieved for the Cr-PILC is not stable at high temperatures. Volzone [29] reported a decrease of the specific micropore volume as well as the presence of Cr_2O_3 when the solids were heated at temperatures above 420 °C in the presence of oxygen. Hopkins et al. [19] reported for Cr-PILC a d_{001} value of 15.4 Å stable up to 300 °C. The structure of the solid is more stable when the calcination is performed in inert atmosphere instead of air [30,31]. Zhao et al. [25] prepared the pillaring solution using both Al and Cr and showed that thermal stability of the PILC reduced with increasing of Cr/Al ratio. Toranzo et al. [27] prepared Al–Cr mixed pillars by basic co-hydrolysis of their salts. Tomul and Balci [32] prepared Al–Cr-PILCs mixing different amounts of solutions containing each of the hydroxylated species; the resulting solutions were aged before use.

Tzou and Pinnavaia [33] and Moini et al. [34] reported good catalytic activity for Cr-PILCs in the reaction of dehydrogenation of cyclohexane to produce benzene. Mata et al. [28] reported the catalytic activity in propene oxidation of Al–Cr-PILCs prepared using oligomers obtained by co-hydrolysis of the corresponding metal chlorides. Kar et al. [35] used Cr-PILCs as catalysts for octahydroxanthenes synthesis in solvent free conditions. Catalytic activity in oxidative dehydrogenation of propane (ODP) of rare earth phosphates supported on Al-PILCs is reported by De Los Santos et al. [36] verifying the highest propylene yields in the temperature range from 400 °C to 600 °C.

To improve thermal stability of Cr-PILCs different preparation routes have been proposed: (a) the co-hydrolysis of a solution containing aluminum and chromium salts at different Al/Cr ratios [25,28], the presence of aluminum in the pillaring solution is proposed to improve thermal stability of the PILC; (b) the hydrolysis of the Al_{13} Keggin polycation in the presence of a chromium salt [26], it has been proposed that chromium can replace aluminum during hydrolysis. In any case no conclusive evidence of mixed species is presented.

The aim of this study was to obtain new and cheap catalysts by pillaring of a Uruguayan montmorillonte with high catalytic activity in the oxidative dehydrogenation of propane. Chromium polyhydroxy cations and Al_{13} were prepared separately. Solutions containing either one of them or a mixture (Cr/Al molar ratio equal to 1) were used for pillaring a montmorillonite. Structural and textural properties of the PILCs were determined and their catalytic activity in ODP was evaluated in the temperature range from 350 °C to 450 °C.

2. Materials and methods

2.1. Starting material

A raw mineral extracted from Bañado de Medina (32° 23′ 0″ South, 54° 21′ 0″ West), Uruguay, was used. Over 80% of it is constituted by a calcium-rich montmorillonite with low sodium and potassium content [37]. Cation exchange capacity (CEC) of the mineral, as determined by the ammonium acetate method (1 M and pH = 7), was 1.12 meq per gram of the dry clay. The interlayer cations were analyzed by atomic absorption spectroscopy and atomic emission spectroscopy. The results in meq/g are as follows: Ca^{+2} 0.82; Mg^{+2} 0.29; Na^{+} 0.012; K^{+} 0.002 [38]. The raw mineral was oven dried at 110 °C for 24 h, ground and sieved. The fraction with aggregates size less than 250 μm was selected and named as M.

2.2. Preparation of catalysts

The solid M was exchanged with solutions containing Cr and/or Al hydroxylated species.

Al-polyhydroxycation solution was prepared from a 0.1 M $AlCl_3$ solution over which a 0.2 M solution of NaOH was slowly added while vigorous stirring was kept. Volumes were selected to give a final molar ratio OH^-/Al^{3+} of 2. The resulting solution was aged for one hour at 50 °C [39]. According to Bottero [40] in those conditions, the 95% of the aluminum is embodied in the Al_{13} cation.

Cr-polyhydroxycation solution was prepared from a 0.1 M $Cr(NO_3)_3$ solution over which a 0.2 M solution of NaOH was slowly added while vigorous stirring was kept. Volumes were selected in order to attain a final molar ratio OH^-/Cr^{3+} of 2. The solution was aged for 24 h at 60 °C [41].

A third solution was obtained by mixing equal volumes of the above aged solutions, resulting in a molar ratio $Cr^{3+}/Al^{3+} = 1$.

Each of the three solutions was added to 10% (w/w) slurry of the solid M. In all cases the volume of the intercalating solution was the necessary to achieve a ratio of 10 mmol of total metal per gram of dry clay and the contact time was 2 h. The resulting solids were separated by filtration and repeatedly washed with deionized water. The exchanged clays obtained (M-samples) were named as Al–M, Cr–M and Al–Cr–M according to the intercalating solution used in the preparation. The M-samples were calcined in air in a tubular furnace, Carbolite, CTF-12/65/550, at a heating rate of 1 °C min^{-1} up to 450 °C, and maintained at this temperature for 2 h. The PILCs thus obtained were identified as Al–C, Cr–C and Al–Cr–C, according

to the intercalating solution used in the preparation. M sample calcined in the same conditions was named as M-450.

2.3. Characterization of solids

A JEOL JS M-5900LV scanning electron microscope, operated at 20 kV was used to obtain SEM microphotographs. The elemental composition of selected zones of the samples was determined by energy dispersive spectrometry with a NORAN Instruments EDS-vantage probe.

Differential thermal analysis (DTA) and thermogravimetric analysis (TGA) for M and M-samples were performed on NETZSCH409 equipment from room temperature and up to 1000 °C in air atmosphere and at a heating rate of 10 °C min^{-1}.

FTIR spectra (4000–400 cm^{-1}) of M and the catalysts were measured as KBr pellets with an IRPrestige-21/FTIR-8400S instrument.

The samples were characterized by X-ray diffraction (XRD) on Philips equipment with 3710 controller and 3020 goniometer, operated at 40 kV and 20 mA using a Ni-filter and Cu Kα radiation in the 2θ degrees range from 3 to 65. Spacings were derived using Bragg's law.

The adsorption–desorption nitrogen isotherms were determined at −196 °C using a Quantachrome, Autosorb-1 equipment, suitable for micropore analysis. Samples were outgassed at 250 °C to a residual pressure below 10 mPa. The specific surface area (S_{BET}) was determined applying the BET model [42] to adsorption data in the p/p^o range that allowed fine adjustment of them. The specific total pore volume (V_T) was calculated, unless otherwise indicated, after the gas adsorption at a relative pressure of 0.95 that was converted to liquid volume using a value of 0.808 g cm^{-3} for the density of the adsorbed nitrogen [43]. The specific micropore volume ($V_{\mu p}$) was determined using the Dubinin–Radushkevich model [43]. The specific external surface area (S_{ext}) and specific micropore surface area ($S_{\mu p}$) were determined applying the t-plot to adsorption data in the relative pressure range from 0.85 to 0.95 [44].

2.4. Catalytic evaluation

The catalytic activity of the solids in the ODP was studied in a "U"-formed fixed bed reactor, built in natural quartz tube, with external diameter of 8 mm and 1 mm wall thickness. The catalyst bed occupied approximately 2 cm in one branch of the reactor. The free volume (pre and post the catalytic bed) was filled with quartz chips in order to minimize the contribution of the homogeneous reactions to the process. In a blank run at 450 °C, the catalytic activity of the reactor full-packed with quartz chips was verified to be negligible.

The reaction gas mixture was 10% in C_3H_8, 10% in O_2 and 80% in Ar (mole percentages) at a total flow of 50 mL min^{-1} measured at 22 °C. The catalytic tests were conducted at atmospheric pressure using 0.5 g of the catalyst. The catalysts were activated at 450 °C for 30 min under Ar flow (40 mL min^{-1}) and the catalytic activity was determined at 350 °C, 400 °C and 450 °C. After 45 min at each temperature a sample of the outlet gas mixture was extracted and analyzed by gas chromatography. The results are presented as C_3H_8 conversion, selectivity to the products CO_2 and C_3H_6. The yield of C_3H_6 was determined as the product of C_3H_8 conversion and C_3H_6 selectivity. Chromatographic relative error was less than 5% and carbon balance was found, in all determinations, to be 100 ± 5%.

3. Results and discussion

SEM microphotographs are shown in Fig. 1 for the catalysts and the host clay. The lamellar structure of the host clay can be appreciated and it is retained in the Cr–C. For the catalysts containing aluminum a more agglomerate structure is observed.

Atomic percentages for the main elements, Si, Al and Cr, were determined by EDS at various zones of the sample. As they were concordant average values are presented in Table 1. Silicon amount –being the only one that is not modified during the preparation– was taken as reference for determination of the atomic ratios.

Al/Si ratio is indicative of the amount of aluminum incorporated by the Keggin ion during the preparation of the solid. The value obtained for the M sample increases almost twice in the Al–C, does not change significantly for the Cr–C and increases only a 17% for the Al–Cr–C. It is worth noting the scarce amount of aluminum incorporated in the Al–Cr–C catalyst, which suggest a strong competence of chromium hydroxylated species during the exchange preparation step. Cr/Si ratios for Al–Cr–C and Cr–C are, considering method uncertainty, the same, even when chromium concentration in the pillaring solution was different (5 mmol g^{-1} for the Al–Cr–C and 10 mmol g^{-1} for the Cr–C). Similar atomic ratios can be derived from mass percentages presented by Tomul and Balci [32] which also support the idea of the high competence of chromium over aluminum during the exchange step of the preparation method.

Thermogram patterns (DTA) for M and M-samples are shown in Fig. 2. An endothermic peak around 170 °C for all the samples is ascribed to the release of water adsorbed on the clay surface and associated to the exchangeable cations located in the interlayer space [45]. The shape of this peak for the M-samples differs from that for M sample, due to the different cations in the interlayer space. In fact, Ca^{2+}, Mg^{2+} and Na^{+} present in M were substituted by the polymeric species OH–Al and/or OH–Cr during the cation exchange step of the pillaring process. The endothermic peak for the sample M is located at 170 °C and shifts to 172 °C, 167 °C and 161 °C, respectively, for Al–M, Al–Cr–M and Cr–M. It is worth noting that the dehydration temperature decreases in the samples as Cr/Al molar ratio increases, suggesting that the hydration water is more loosely bound in the samples intercalated with chromium species. A second endothermic peak centered at 678 °C in the thermogram of the sample M (Fig. 2) is assigned to the release of the hydroxyl groups of the montmorillonite [45]. The dehydroxylation temperature for are 650 °C, 647 °C and 644 °C, respectively for Al–M, Al–Cr–M and Cr–M so it decreases as Cr/Al molar ratio increases.

The inclusion of hydroxylated species between the montmorillonite layers resulted in the presence of exothermic peaks between 300 °C and 500 °C (Fig. 2) attributable to the formation of the oxidic phases of aluminum and chromium [41,46].

The small endo-exothermic S-shaped peaks in the range from 890 °C to 990 °C correspond to changes in the montmorillonite structure generating new phases [45]. Intercalation of the aluminum and/or chromium species caused the shift of these peaks to higher temperatures indicating an increase of the thermal stability. The endothermic peak at 890 °C shifted to 942 °C for the solid to which only chromium species were incorporated.

The thermogravimetric analysis diagrams (TGA) for M and M-samples are shown in Fig. 3. A noticeable difference in the pattern obtained for the M sample and those for the exchanged ones (Al–M, Cr–M and Al–Cr–M) is observed. The first one shows the characteristic behavior of a montmorillonite with a quite abrupt mass loss up to 250 °C due to water release, either adsorbed on the clay surface or associated to the exchangeable cations in the interlayer space and a second mass change verified in the temperature range from 500 °C to 700 °C is attributed to montmorillonite structural hydroxyl groups that are lost as water. On the other hand for the M-samples the mass loss occurs continuously with increasing temperature up to 700 °C and is assigned also to water release from the OH-polymeric species of aluminum and/or chromium [31].

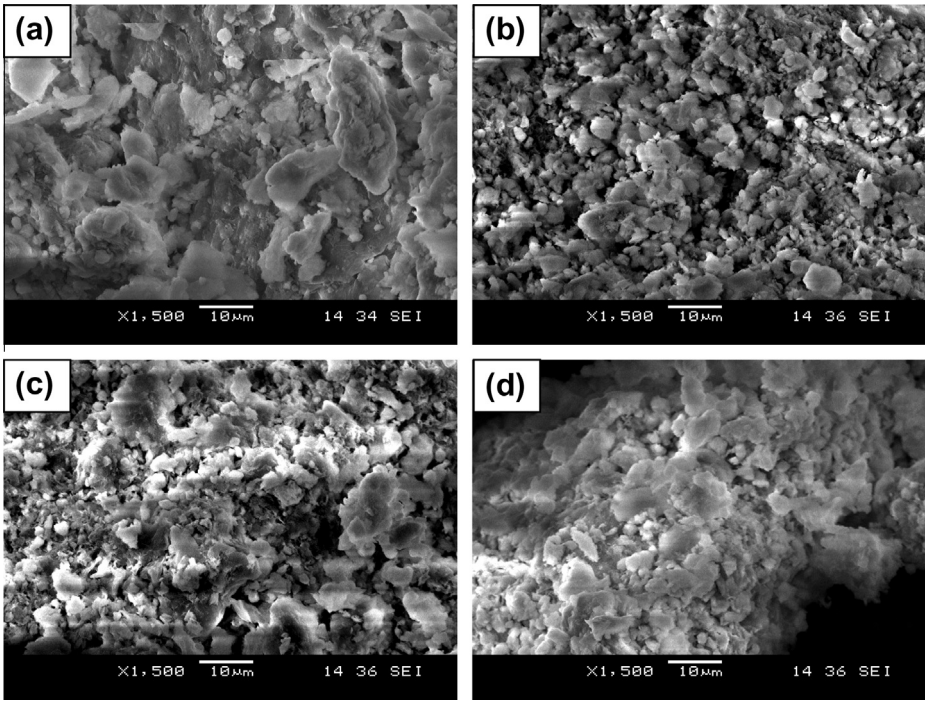

Fig. 1. SEM microphotographs of: (a) host clay, (b) Al–C, (c) Al–Cr–C, (d) Cr–C.

Table 1
Atomic ratios for M-450 and the catalysts determined after EDS data taking silicon as reference.

	M-450	Al–C	Al–Cr–C	Cr–C
Al/Si	0.29	0.49	0.34	0.29
Cr/Si	–	–	0.22	0.22
Cr/Al	–	–	0.66	0.74

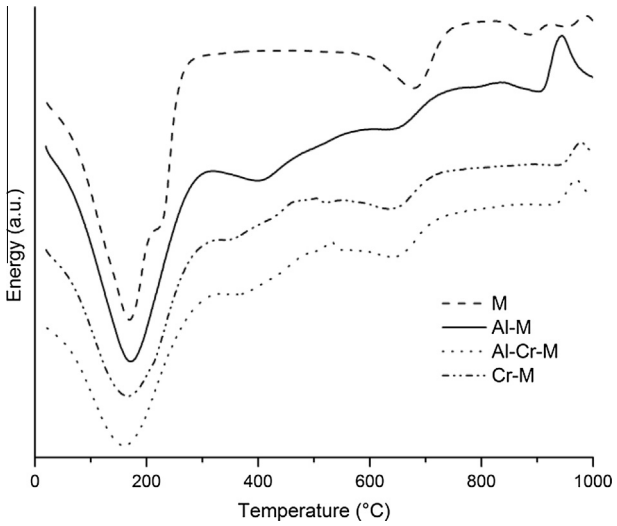

Fig. 2. Thermogram (DTA) for the clay and the M-samples.

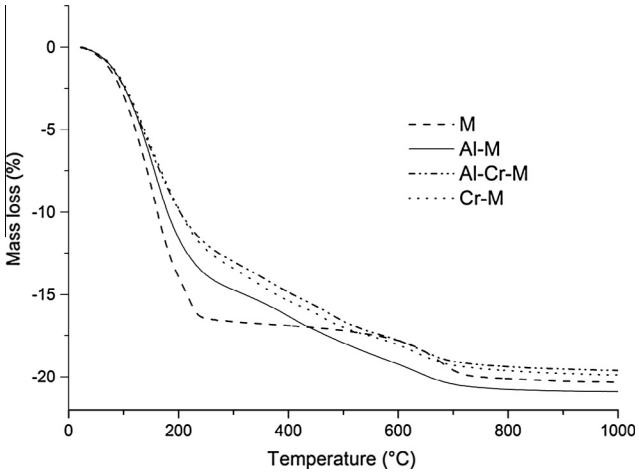

Fig. 3. Thermogram (TGA) for the clay and the M-samples.

The mass loss up to 250 °C observed in the thermogram corresponds to the peak at 170 °C in the DTA diagram, while that verified up to 700 °C does to the peak about 650 °C for the C-samples and at 678 °C for the sample M.

Infrared spectra (Fig. 4) for the host clay, M, shows bands at 3628, 3431, 1110, 1030, 910, 842, 517, 468 cm^{-1} that are typical of montmorillonite, as well as bands at 798 and 626 cm^{-1} corresponding to the presence of small amounts of cristobalite, 695 cm^{-1} (Si–O symmetrical bending vibration) and at 778 cm^{-1} (Si–O stretching vibration) evidencing the occurrence of quartz [47]. The bands at 3628 and 3431 cm^{-1} are respectively assigned to OH-stretching vibration (Al–Al–OH) and OH^- from intercalated water in the montmorillonite. The band at 1634 cm^{-1} is attributed to OH vibration bending of H–O–H. The Si–O–Si stretching parallel and perpendicular vibrations bands at 1030 and at 1110 cm^{-1}, respectively, are observed for all the samples. The bands at 910 and 842 cm^{-1} are respectively assigned to the bending vibrations of Al–Al–OH and Mg–Al–OH groups and they are also observed in the pillared samples, especially for those containing chromium, but at higher wavenumber values 934 and 877 cm^{-1}. This fact would suggest some interaction of the pillaring species with Al–OH and Mg–OH groups of the octahedral sheet of the host clay. This observation reinforces what was observed in the TGA analysis:

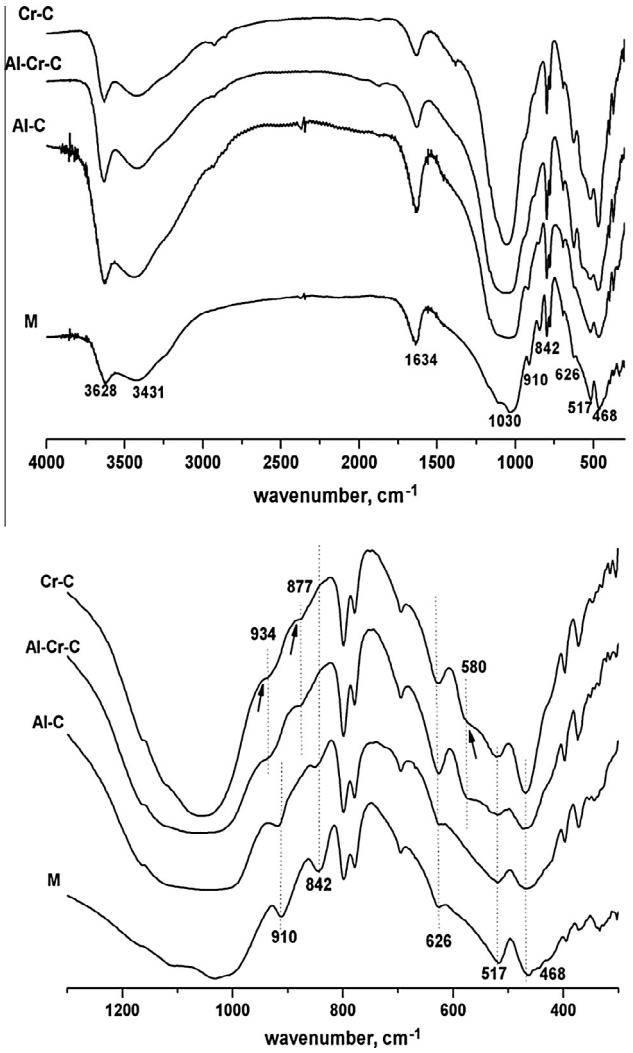

Fig. 4. Infrared spectra for the clay and the catalysts.

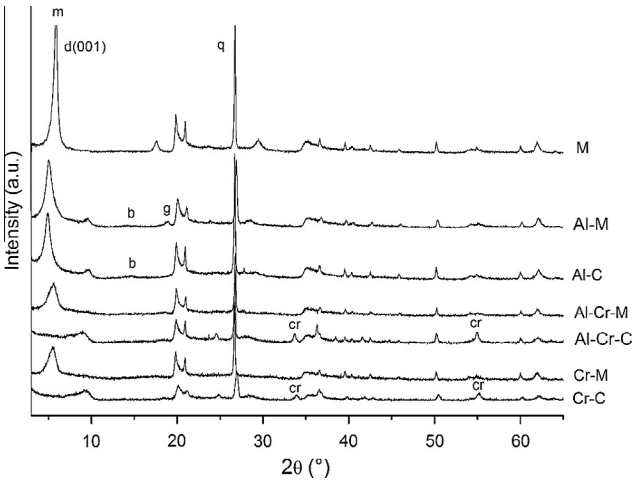

Fig. 5. X-ray Diagrams for the samples prior (M-samples) and after (C-samples) calcination at 450 °C. m: montmorillonite; b: boehmite; cr: Cr_2O_3; g: gibbsite; q: quartz.

in fact the presence of chromium shifts these IR bands to higher wavenumber values, implying lower interaction energy which reflects in the lower temperature at which water loss was observed in the TGA profile. The bands at 517 and 468 cm^{-1} clearly visible in all the spectra correspond to Si–O–Al^{IV} and Si–O–Si structural groups of the host clay. The shoulder at 580 cm^{-1} in the chromium containing samples (Al–Cr–C and Cr–C) are assigned to Cr–O vibration and indicate the presence of Cr(III) [48].

Fig. 5 shows the diffractograms for the starting solid M, the M-samples and the catalysts. The montmorillonitic character of the clay, as well as the presence of quartz impurities, is confirmed by the presence of the sharp and well defined characteristic peaks for these minerals. For the Al–M sample the intercalation of hydroxylated Al species caused an increase of the d_{001} spacing of 14.91 Å for the M sample to 17.70 Å. Considering the minimum spacing for the montmorillonite of 9.8 Å [49] the height of the gallery generated by pillaring can be determined to be of 7.9 Å. This value results intermediate between the crystalline size of the dehydrated cation of Al_{13} determined by Johansson [50] and that in water solution determined by Bottero et al. [51], suggesting that the Al_{13} still retains some of the hydration water at the calcination temperature. The presence of gibbsite, $Al(OH)_3$, is evidenced by a low intensity peak at 4.78 Å, and boehmite, AlO(OH), can be identified by the peak at 6.20 Å although it is barely visible. Calcination at 450 °C of this sample gives the catalyst Al–C and does not alter either the interlamellar spacing of 17.70 Å or the Al-hydroxylated phase corresponding to boehmite species. On the other hand the more hydrated species of gibbsite, $Al(OH)_3$, disappear during the calcination, and the peak corresponding to boehmite increases, as evidenced by XRD.

For the Al–Cr–M sample, in which both hydroxylated species (Al and Cr) were used in the exchange step, a d_{001} spacing of 16.33 Å was determined after XRD diagram. Even when this value is lower than the one achieved when only Al-species were intercalated (Al–M), it is indicative that the oligomer species have been incorporated in the interlayer space. In addition, as this peak for Al–Cr–M is lower and wider than the corresponding one for the Al–M sample, it can be concluded that the simultaneous inclusion of the Al and Cr hydroxylated species gave a less defined spacing, hence a poorer crystalline structure. For this sample the peak corresponding to gibbsite, $Al(OH)_3$, even being wider than that observed for the Al–M sample, is also shown, indicating that Al_{13} species have been incorporated during the exchange step. Calcination of the Al–Cr–M sample at 450 °C results in the Al–Cr–C catalyst, which diffractogram shows a low intensive and broad peak evidencing the poorer crystallinity of the solid and corresponding to a d_{001} spacing of 9.8 Å, characteristic for a non-pillared dehydrated montmorillonite. The heat treatment caused the appearance of the Cr_2O_3 phase evidenced by the peaks identified in Fig. 5, which are not observed in the corresponding exchanged clay (Al–Cr–M).

For the Cr–M sample a d_{001} spacing of 16.33 Å is determined from the XRD diagram, being equal to that of the Al–Cr–M sample and leaving an interlayer space of 6.5 Å. After Volzone's indication of chromium polycations height: 4.0 Å for the dimer, 5.0 Å for the trimer and 6.5 Å for the tetramer [29] it can be postulated that in this case the tetrameric chromium polycation is the intercalated species. However, treatment at 450 °C, at which the Cr–C catalyst is obtained, caused the d_{001} spacing to collapse to 9.5 Å, slightly lower than the observed for the Al–Cr–C sample. Toranzo et al. [27] reported a d_{001} spacing of 18.9 Å for a saponite intercalated with chromium polycations and verified that after calcination at 300 °C it reduces to the value corresponding to the non-pillared dehydrated saponite, as was verified here for the montmorillonite. Also the characteristic peak for Cr_2O_3, not observed for the Cr–M sample, is present in the diffractogram for Cr–C, indicating that this species has been formed during calcination.

It is worth noting that the d_{001} spacing for Al–Cr–C and Cr–C correspond to the sheet height of the montmorillonite, i.e. that

even when the Cr_2O_3 phase can be identified by XRD it has not contributed to the clay layers separation acting as pillars. On the other hand either stability of Al_{13} pillars has been compromised by the presence of Cr-species or the amount of aluminum incorporated has been so low that Al-pillaring is not evidenced by XRD. Comparison of the Al/Si and Cr/Si molar ratios for these samples (Table 1) evidenced the lower amount of Al incorporated in the Al–Cr–C catalyst.

Nitrogen adsorption isotherms (Fig. 6) were determined for the catalysts and for the clay that was previously calcined at 450 °C (M-450). At low relative pressures an important adsorption is observed for the Al–C sample, being significantly lower for Al–Cr-PILC, Cr-PILC and M-450. This is indicative of the microporous character of the catalyst obtained by pillaring the montmorillonite with aluminum polyoxocations different from those in which chromium species have been included. This fact is coincident with the d_{001} spacing values derived from XRD analysis for the Al–Cr–C and Cr–C samples.

Table 2 summarizes the textural parameters of the solids derived from nitrogen adsorption data. For Al–C, a fine adjustment to BET model was obtained for the adsorption data in the relative pressures range from 0.007 to 0.1. For the other solids, and in accordance to the non-microporous character of them, a fine adjustment to BET model was obtained for adsorption data in the relative pressure range from 0.05 to 0.25. The specific surface area (S_{BET}) of Al–C, the clay exchanged with aluminum polioxocations and calcined at 450 °C, is eleven fold higher than that of M-450. However, the specific surface area of Cr–C is less than double than the one of M-450, indicating the lower thermal stability of the chromium pillars with respect to aluminum pillars and corroborating what was observed after XRD analysis. Indeed, the d_{001} spacing corresponds to pore diameter in the range of micropore and a diminution of it involves a decrease of the adsorption volume in the interlamellar space of the PILC. As adsorption data considered for BET specific surface area determination include those in the p/p^o range of the isotherm at which micropores are filled, the lower d_{001} spacing results in a minor value of the specific surface area.

For the Al–Cr–C, obtained by exchange of the mineral with the solution containing both polycations and calcined at 450 °C, the specific surface area is only slightly higher than that for Cr–C, suggesting that aluminum has barely contributed to increase thermal stability of the Cr–C. A strong competition between chromium and aluminum polycations to replace the interlayer cations could be responsible for the exclusion of aluminum species from the interlayer space as previously proposed in the text.

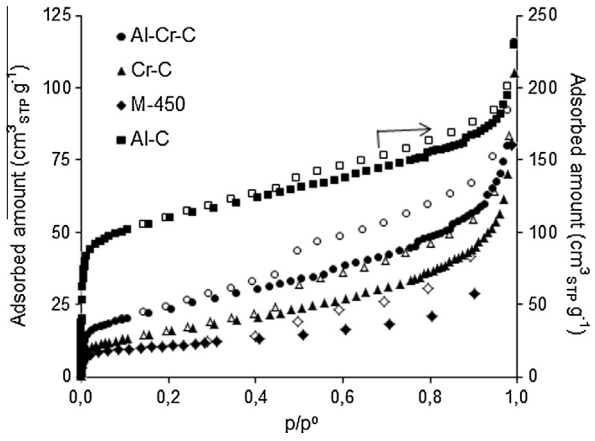

Fig. 6. Nitrogen adsorption–desorption isotherms at −196 °C. Filled symbols: adsorption, open symbols: desorption. Isotherm for Al–Cr–C is referred to the right hand *y*-axis.

Table 2
Textural parameters derived from nitrogen adsorption data.

Solid	V_T ($cm^3\ g^{-1}$)	$V_{\mu p}$ ($cm^3\ g^{-1}$)	S_{BET} ($m^2\ g^{-1}$)	S_{ext} ($m^2\ g^{-1}$)	$S_{\mu p}$ ($m^2\ g^{-1}$)
M-450	0.124	0.000	37	37	0
Al–C	0.276	0.167	401	59	347
Al–Cr–C	0.104	0.034	84	44	45
Cr–C	0.083	0.022	57	51	11

The specific micropore volume ($V_{\mu p}$) for Al–C was of 0.167 $cm^3\ g^{-1}$, corresponding to 60% of the specific total pore volume determined from the adsorption data at a relative pressure of 0.95. For Al–Cr–C and Cr–C the specific micropore volume represents the 33% and the 25% of each one of the specific total pore volume. These results suggest a higher contribution of aluminum pillars to generate the microporous structure. The specific external surface area (S_{ext}) for the calcined M sample (M-450) is identical to the S_{BET} surface area, emphasizing the non-microporous character of the sample. For the catalysts Al–C, Al–Cr–C and Cr–C the external surface area represents, respectively, 15%, 52% and 90% of the S_{BET} value. As at intermediate relative pressures the adsorption branch of the isotherms for all the samples is parallel to *x*-axis, the difference between S_{BET} and S_{ext} is related to the presence of micropores. The above mentioned percentages indicate that an important microporous network was developed in the Al–C catalyst but not in Al–Cr–C and Cr–C samples, in accordance with what was observed for specific total and micropore volumes and was evidenced by XRD diagrams.

The results of the catalytic test versus temperature are presented as C_3H_8 conversion and selectivity to CO_2 and C_3H_6 (Table 3). Propane conversions between 20% and 27% are obtained with the catalysts Al–Cr–C and Cr–C, and are significantly higher than those achieved with the catalyst without chromium, Al–C, evidencing the catalytic role of chromium. C_3H_8 conversion attained with the M-450 sample is similar to that obtained with the Al–C catalyst at 350 °C and 400 °C, but is lower at 450 °C. Catalytic activity of the Al–C catalyst is markedly influenced by temperature as C_3H_8 conversion values indicate; however, temperature influence is milder for the Cr–C catalyst, while for Al–Cr–C an increased temperature hardly influences C_3H_8 conversion values within the temperature range of the experiment.

For all catalysts the reaction products are just CO_2 and C_3H_6. The fact of not having detected CO, CH_4 and C_2H_4 is reasonable because they are generated by reactions which occur at temperatures above 500 °C not used in this study.

With respect to C_3H_6 selectivity for Al–Cr–C and Cr–C catalysts a slight increase with temperature is observed, a trend that has been reported for others Cr-containing catalysts [6,52]. For Al–C catalyst an increase in C_3H_6 selectivity was observed when temperature increases from 350 °C to 400 °C, decreasing then abruptly when catalytic test was performed at 450 °C, temperature at which CO_2 formation is kinetically and thermodynamically favored and thus increasing CO_2 selectivity. This performance is typical for most of the catalytic systems used in ODP [1].

Propylene yield for the catalysts is shown as function of the temperature at which the catalytic test was performed (Table 3). At all temperatures the highest C_3H_6 yield is attained with the catalysts containing chromium, Al–Cr–C and Cr–C, being slightly higher for the one containing both metals. It should be noted that except at 350 °C, C_3H_6 yield obtained with Al–C catalyst is higher than that attained with M-450 catalyst. The highest C_3H_6 yields, 10.3% and 9.5%, were achieved at 450 °C with Al–Cr–C and Cr–C respectively. These values are nearly double than the ones obtained with the Al–C catalyst, and are specially outstanding since at temperatures as low as the ones' used in the present study, most

Table 3
C_3H_8 conversion, selectivity to CO_2 and C_3H_6 and C_3H_6 yield as function of the temperature.

Solid	T (°C)	C_3H_8 conversion (%)	Selectivity (%)		C_3H_6 yield (%)
			CO_2	C_3H_6	
M-450	350	2.4	0	100	2.4
	400	3.9	33	67	2.6
	450	4.8	35	65	3.1
Al–C	350	3.1	34	66	2.1
	400	3.8	28	72	2.7
	450	9.4	49	51	4.8
Al–Cr–C	350	25.5	63	37	9.3
	400	26.2	64	36	9.5
	450	26.7	62	38	10.3
Cr–C	350	19.9	68	32	6.3
	400	25.1	66	34	8.4
	450	26.3	64	36	9.5

catalysts are inactive in ODP [1]. Besides, yields over 7% have not been reported for Al-PILCs even at temperatures as high as 600 °C [36].

It is highly remarkable that even at 350 °C a propylene yield of 9.3% was obtained with the Al–Cr–C catalyst, since most of the catalytic systems for ODP require higher temperatures to attain such high values [1]. Indeed there is no propylene yield above 10% reported for temperatures in the range of 350–450 °C. On the other hand, although propene yields above 20% were reported for a few catalysts in all cases the working temperatures were higher than 500 °C [1]. It is also worth noting that for this catalyst propylene yield results practically constant within the temperature range here studied. It is also interesting to remark that these values results of constant values for both propane conversion and propylene selectivity.

The highest propylene yield obtained with Al–Cr–C is possible to be related to differences in the textural properties and/or the composition of the catalyst. The higher propylene yield for Al–Cr–C catalyst compared to that obtained with the Cr–C one can be related not only to the higher specific surface area (65%) but also to the higher specific pore volume (48%). The higher propylene yield for Al–Cr–C compared to that obtained with the Al–C one is related to the presence of chromium as catalytic species. Considering catalysts composition, the present results agree with those reported for other Cr_2O_3 supported catalysts in ODP. For a series of chromium oxide-based catalysts Jibril [53] has reported a correlation between the nature of the support and product distribution in ODP, concluding that catalyst involving Cr–Al–O interactions were slightly more selective to propylene than those containing Cr–Si–O interactions, which appears as responsible for the higher CO_2 selectivity. The present results on CO_2 and propylene selectivity for Cr–C and Al–Cr–C are in accordance with the data reported by Jibril [53]. Indeed the Cr–C catalyst is slightly more selective to CO_2 while the Al–Cr–C one is to propylene, a fact that can be explained by the presence of chromium and aluminum in the interlayer giving the Cr–Al–O interactions reported by Jibril [53] as responsible for higher propylene selectivity.

The catalytic activity evidenced here for chromium has been assigned for diverse chromium containing catalysts to the presence of Cr (VI): pillared saponites [28] and chromium oxide supported on alumina [7,8,54], on silica [9], or modified silicalite [12]. In this study we have verified by XRD the presence of chromium in the fresh catalyst, which was calcined at 450 °C, but only as Cr_2O_3. Other author using similar systems and varied techniques for the characterization of the solids have confirmed the presence of Cr(III), Cr(V) and Cr(VI) species [27]. Labajos and Rives [55] reported Cr(VI) as the only metal species in solids containing chromium that were calcined in a oxidant atmosphere at 400 °C and verified that its amount decreased strongly when the calcination temperature increased to 500 °C. In turn the increase of chromium load almost exclusively lead to the formation of Cr_2O_3 [10,28]. In our case both premises are fulfilled, i.e. high load of chromium and calcination at 450 °C. Besides considering the oxidant character of the reaction mixture is not to exclude that in the conditions of the catalytic assay the oxidation of Cr_2O_3 on the catalyst surface gives rise to the Cr(VI) species to which the catalytic activity is assigned.

Long-term reactivity for the catalysts that allowed the highest propene yield, Al–Cr–C and Cr–C, was checked at 450 °C during 10 h after being activated as previously described. The outlet gas mixture was sampled and chromatographically analyzed every 45 min. For both catalysts and considering the experimental error, a constant propene yield was verified.

It is interesting to note that even when propene yield attained was about 10%, propane conversion was about 25%, i.e. the outlet gas mixture contains a propane/propene molar ratio between 5 and 7. Propane-propene separation, allowing to re-inject the unconverted propane in the reaction mixture, has been considered one the most challenging aspects of propene production in the petrochemical industry due the similar physico-chemical properties of both molecules. Recent advances in this topic have been reported based either on adsorption processes on modified zeolites [56] and metal–organic frameworks [57,58] or on reactive absorption on Ag^+-ionic liquid media [59].

4. Conclusions

The solids obtained by pillaring the montmorillonitic clay with aluminum and/or chromium, Al–C, Al–Cr–C and Cr–C, showed significantly differences of their textural parameters, specific surface area and micropore volume as well as interlamellar spacing, evaluated after nitrogen adsorption and X-ray diffraction data, respectively.

All the tested catalysts were active in ODP. The highest yield to propylene was obtained with the catalyst Al–Cr–C, being very noticeable the difference with other catalysts' yield especially at low temperature. The presence of both chromium and aluminum in the interlayer space of the PILC would generate the Cr–Al–O interactions that Jibril [46] reports as to be responsible for high propylene selectivity. In addition, the high propane conversion obtained with this catalyst results in the highest propylene yield verified in this study.

The highest propylene yield (10.3%) was obtained with the Al–Cr–C catalyst at 450 °C, but it is remarkable that even at temperatures as low as 350 °C a propylene yield of 9.3% is highly promissory.

Acknowledgements

Comisión Sectorial de Investigación Científica (CSIC), Universidad de la República, Uruguay and Consejo Nacional de Investigaciones Científicas y Técnicas (CONICET), Argentina, for financial support.

Dra. Zulema Coppes for the language revision.

References

[1] F. Cavani, N. Ballarini, A. Cericola, Oxidative dehydrogenation of ethane and propane: how far from commercial implementation?, Catal Today 127 (2007) 113–131.
[2] E.V. Shelepova, A.A. Vedyagin, I.V. Mishacov, A.S. Noskov, Mathematical modeling of the propane dehydrogenation process in the catalytic membrane reactor, Chem. Eng. J. 176–177 (2011) 151–157.
[3] B.A. Jibril, A.Y. Atta, K. Melghit, Z.M. el-Hadi, A.H. Al-Muhtaseb, Performance of supported $Mg_{0.15}V_2O_{5.15}2.4H_2O$ nanowires in Dehydrogenetion of propane, Chem. Eng. J. 193–194 (2012) 391–395.
[4] Y. Zhang, Y. Zhou, M. Tang, X. Liu, Y. Duan, Effect of La calcination temperature on catalytic performance of PtSnNaLa/ZSM-5 catalyst for propane dehydrogenation, Chem. Eng. J. 181–182 (2012) 530–537.
[5] M.M. Bhasin, J.H. McCain, B.V. Vora, T. Imai, P.R. Pujadó, Dehydrogenation and oxydehydrogenation of paraffin to olefins, Appl. Catal. A 221 (2001) 397–419.
[6] M. Cherian, M.S. Rao, W. Yang, J. Jehng, A.M. Hirt, G. Deo, Oxidative dehydrogenation of propane over Cr_2O_3–Al_2O_3 and Cr_2O_3 catalysts: effects of loading, precursor and surface area, Appl. Catal. A 233 (2002) 21–33.
[7] S.J. Khatib, J.L.G. Fierro, M.A. Bañares, Effect of phosphorus additive on the surface chromium oxide species on alumina for propane oxidation to propylene, Top. Catal. 52 (2009) 1459–1469.
[8] E. Rombi, D. Gazzoli, M.G. Cutrufello, S. De Rossi, I. Ferino, Modifications induced by potassium addition on chromia/alumina catalysts and their influence on the catalytic activity for the oxidative dehydrogenation of propane, Appl. Surf. Sci. 256 (2010) 5576–5580.
[9] M.A. Botavina, G. Martra, Yu.A. Agafonov, N.A. Gaidai, N.V. Nekrasov, D.V. Trushin, S. Coluccia, A.L. Lapidus, Oxidative dehydrogenation of C3–C4 paraffins in the presence CO_2 over of CrO_x/SiO_2 catalysts, Appl. Catal. A 347 (2008) 126–132.
[10] M.A. Botavina, C. Evangelisti, Yu.A. Agafonnov, N.A. Gaidai, N. Panziera, A.L. Lapidus, CrO_x/SiO_2 catalysts preparared by metal vapour synthesis: physical–chemical characterization and functional testing in oxidative dehydrogenation of propane, Chem. Eng. J. 166 (2011) 1132–1138.
[11] F. Ma, S. Chen, Y. Wang, F. Chen, W. Lu, Characterization of redox and acid properties of mesoporous Cr–TiO_2 and its efficient performance for oxidative dehydrogenation of propane, Appl. Catal. A 427–428 (2012) 145–154.
[12] Q. Zhu, M. Takiguchi, T. Setoyama, T. Yokoi, J.N. Kondo, T. Tatsumi, Oxidative dehydrogenation of propane with CO_2 over Cr/H[B]MFI catalysts, Catal. Lett. 141 (2011) 670–677.
[13] D.E.W. Vaughan, Pillared clays – a historical perspective, Catal. Today 2 (1988) 187–198.
[14] Z. Ding, J.T. Kloprogge, R.L. Frost, G.Q. Lu, H.Y. Zhu, Porous clays and pillared clays-based catalysts. Part 2: A review of the catalytic and molecular sieve applications, J. Porous Mater. 8 (2001) 273–293.
[15] A. Gil, L.M. Gandía, Recent advances in the synthesis and catalytic applications of pillared clays, Catal. Rev. – Sci. Eng. 42 (2000) 145–212.
[16] J. Herney-Ramirez, M.A. Vicente, L.M. Madeira, Heterogeneous photo-Fenton oxidation with pillared clay-based catalysis for wastewater treatment. A review, Appl. Catal. B 98 (2010) 10–26.
[17] S.M. Bradley, R.A. Kydd, Ga_{13}, Al_{13}, $GaAl_{12}$ and chromium-pillared montmorillonites: acidity and reactivity for cumene conversion, J. Catal. 141 (1993) 239–249.
[18] G.W. Brindley, S. Yamanaka, A study of hydroxy-chromium montmorillonites and the form of the hydroxy-chromium polymers, Am. Mineral. 64 (1979) 830–835.
[19] P.D. Hopkins, B.L. Meyer, D.M. Van Duch, US Patent 4452910, 1984.
[20] R.M. Carr, Hydration states of interlamellar chromium ions in montmorillonite, Clays Clay Miner. 33 (1985) 357–361.
[21] T.J. Pinnavaia, M.S. Tzou, S.D. Landau, New chromia pillared clay catalysts, J. Am. Chem. Soc. 107 (1985) 4783–4785.
[22] K.A. Carrado, A. Kostapapas, S.L. Suib, R.W. Coughlin, Physical and chemical stabilities of pillared clays containing transition metal ions, Solid State Ionics 22 (1986) 117–125.
[23] K.A. Carrado, S.L. Suib, N.D. Skoularikis, R.W. Coughlin, Chromium(III)-doped pillared clays (PILC's), Inorg. Chem. 25 (1986) 4217–4221.
[24] N.D. Skoularikis, R.W. Coughlin, A. Kostapapas, K. Carrado, S.L. Suib, Catalytic performance of iron(III) and chromium(III) exchanged pillared clays, Appl. Catal. 39 (1988) 61–76.
[25] D. Zhao, Y. Yang, X. Guo, Synthesis and characterization of hydroxy-CrAl pillared clays, Zeolites 15 (1995) 58–66.
[26] L. Storaro, R. Ganzerla, M. Lenarda, R. Zanoni, A. Jiménez López, P. Olivera-Pastor, E. Rodríguez-Castellón, Catalytic behaviour of chromium-doped alumina pillared clay materials fo the vapor phase deep oxidation of chlorinated hydrocarbons, J. Mol. Catal. A: Chem. 115 (1997) 329–338.
[27] R. Toranzo, M.A. Vicente, M.A. Bañares-Muñoz, Pillaring of a saponite with aluminum–chromium oligomers. Characterization of the solids obtained, Chem. Mater. 9 (1997) 1829–1836.
[28] G. Mata, R. Trujillano, M.A. Vicente, C. Belver, M. Frenández-García, S.A. Korili, A. Gil, Chromium-saponite clay catalysts: preparation, characterization and catalytic performance in propene oxidation, Appl. Catal. A 327 (2007) 1–12.
[29] C. Volzone, Hydroxy-chromium smectite: influence of Cr added, Clays Clay Miner. 43 (1995) 377–382.
[30] C. Volzone, Síntesis y Caracterización de Esmectitas con Pilares de Cromo (Cr-PILCs), Tésis Doctoral, Facultad de Ingeniería, Universidad Nacional de la Plata-Argentina, 1997.
[31] C. Volzone, A.M. Cesio, Changes in OH–Cr montmorillonite after heating in air and nitrogen atmospheres, Mater. Chem. Phys. 79 (2003) 98–102.
[32] F. Tomul, S. Balci, Characterization of Al, Cr-pillared clays and Co oxidation, Appl. Clay Sci. 43 (2009) 13–20.
[33] M.S. Tzou, T.J. Pinnavaia, Chromia pillared clay, Catal. Today 2 (1988) 243–259.
[34] A. Moini, T.D. Brewer, M.-S. Tzou, S.D. Landau, B.-K. Teo, T.J. Pinnavaia, Reactive Cr–O Sites. Catalytic Properties of Chromia-Pillared Montmorillonite and Preliminary Study Results, in: L.M. Coyne, S.W.S. McKeever, D.F. Blake (Eds.), Spectroscopic Characterization of Minerals and Their Surfaces, ACS Symposium Series, Washington, 1990, pp. 455–467.
[35] P. Kar, S. Samantaray, B.G. Mishra, Catalysitc application of chromia-pillared montmorillonite towards environmentally synthesis of actahydroxanthenes, React. Kinet. Mech. Cat. (2012) 1–11.
[36] C. De Los Santos, P. Yeste Sigüenza, M. Sergio, J. Castiglioni, Oxidative dehydrogenation of propane by rare earth phosphates supported on Al-PILC, Avances en Ciencia e Ingeniería 3 (2012) 103–115.
[37] W. Diano, R. Rubino, M. Sergio, Al-pillared montmorillonite: preparation from concentrated slurries of homoionic Ca clay, characterization and thermal stability, Microporous Mesoporous Mater. 2 (1994) 179–184.
[38] M. Sergio, S. Cardozo, C. Froche, M. Bentancor, M. Musso, W. Diano, Some structure properties of an Al-PILC according to the grinding of the starting montmorillonitic mineral, in: E.A. Domínguez, G.R. Mas, F. Cravero (Eds.), A Clay Odyssey, Elsevier, Nederland, pp. 639–646.
[39] M. Sergio, M. Musso, J. Medina, W. Diano, Aluminium-pillaring of a montmorillonitic clay: textural properties as a function of the starting particle size, Adv. In Technol. Mater. Proc. J. 8 (2006) 5–12.
[40] J.Y. Bottero, J.M. Cases, F. Fiessinger, J.E. Poirier, Studies of hydrolyzed aluminum chloride solutions. 1. Nature of aluminum species and composition of aqueous solutions, J. Phys. Chem. 84 (1980) 2933–2939.
[41] C. Volzone, M.A. Cesio, Structural modifications of OH–Cr-smectites after thermal treatment up to 1000 °C, Mater. Chem. Phys. 48 (1997) 216–219.
[42] S. Brunauer, P.H. Emmett, E. Teller, Adsorption of gases in multimolecular layers, J. Am. Chem. Soc. 60 (1938) (1938) 309–319.
[43] F. Rouquerol, J. Rouquerol, K. Sing, Adsorption by Powders and Porous Solids, Academic Press, London, 1999.
[44] S.J. Gregg, K.S.W. Sing, Adsorption, Surface Area and Porosity, second ed., Academic Press Inc., London, 1991.
[45] R.C. Mackenzie, S. Caillère, Thermal analysis DTA, TG, DTG, in: H. van Olphen, J.J. Fripiat (Eds.), Data Handbook for Clay Materials and Other Nonmetallic Minerals, Pergamon Press, Oxford, 1979. 243–243.
[46] C. Volzone, L.B. Garrido, Retention of OH–Al complexes by dioctahedral smectites, Clay Miner. 36 (2001) 115–123.
[47] V.C. Farmer, Infrared spectroscopy in clay mineral studies, Clay Miner. 7 (1968) 373–387.
[48] M. Riad, Influence of magnesium and chromium oxides on the physicochemical properties of gamma-alumina, Appl. Catal. A 327 (2007) 13–21.
[49] H. van Olphen, An Introduction to Clay Colloid Chemistry, 2nd ed., Wiley, New York, 1997.
[50] G. Johanson, On the crystal structures of some basic aluminium salts, Acta Chem. Scand. 14 (1960) 771–773.
[51] J.Y. Bottero, D. Tchoubar, J.M. Cases, F. Fiessinger, Investigation of the hydrolysis of aqueous solutions of aluminum chloride. 2. Nature and structure by small-angle x-ray scattering, J. Phys. Chem. 86 (1982) 3667–3673.
[52] J. Castiglioni, R. Situmeang, R. Kieffer, Comparación de la actividad catalítica de Cromatos y Vanadatos de tierras raras en la Deshidrogenación Oxidativa del Propano, in: Proceedings of XVII Simpósio Iberoamericano de Catálisis, Oporto, Portugal, 2000, pp. 191–192.
[53] B.Y. Jibril, Propane oxidative dehydrogenation over chromium oxide-based catalysts, Appl. Catal. A 264 (2004) 193–202.
[54] M. Cherian, R. Gupta, M.S. Rao, G. Deo, Effect of modifiers on the reactivity of Cr_2O_3/Al_2O_3 and Cr_2O_3/TiO_2 catalysts for the oxidative dehydrogenation of propane, Catal. Lett. 86 (2003) 179–189.
[55] F.M. Labajos, W. Rives, Thermal evolution of chromium(III) ions in hydrotalcite-like compounds, Inorg. Chem. 35 (1996) 5313–5318.
[56] C.A. Grande, J. Gascon, F. Kapteijn, A.E. Rodrigues, Propane/propylene separation with Li-exchanged zeolite 13X, Chem. Eng. J. 160 (2010) 207–214.
[57] M. Jorge, N. Lamia, A.E. Rodrigues, Molecular simulation of propane/propylene separation on the metal–organic framework CuBTC, Colloids Surf. A: Physicochem. Eng. Asp. 357 (2010) 27–34.
[58] A.F.P. Ferreira, J.C. Santos, M.G. Plaza, N. Lamia, J.M. Loureiro, A.E. Rodrigues, Suitability of Cu-BTC extrudates for propane–propylene separation by adsorption processes, Chem. Eng. J. 167 (2011) 1–12.
[59] M. Fallanza, M. González-Miguel, E. Ruiz, A. Ortiz, D. Gorri, J. Palomar, I. Ortiz, Screening of RTILs for propane/propylene separation using COSMO-RS Methodology, Chem. Eng. J. 220 (2013) 284–293.